DEVELOPMENT OF URBAN AND REGIONAL EARTHQUAKE HAZARD MAPS IN THE U.S.

Ivan Wong[1], Walt Silva[2], Susan Olig[1], Mark Dober[1], Doug Wright[1], Patricia Thomas[1], and Nick Gregor[2]

ABSTRACT

Since 1997, we have been developing, in collaboration with state geological surveys, earthquake ground shaking hazard maps at local and regional scales in the U.S. These maps illustrate the intensity and variability of ground shaking at a microzonation scale due to the local site response of both soil and rock. The maps are used in a number of ways such as increasing general public awareness of earthquake hazards, urban planning, selecting facility sites, assisting in mitigation planning for lifelines, aiding emergency preparedness and response, and loss estimation. Both earthquake scenario and/or probabilistic maps generally for return periods of 500 and 2,500 years have been developed. Ground motions are expressed in terms of peak horizontal acceleration and spectral acceleration at 0.2 and 1.0 second.

Introduction

In the past three decades, tremendous advances have been made in identifying and characterizing seismic sources in the western U.S., and in evaluating and quantifying the level of the associated seismic hazards. Many of these advances have resulted from extensive site-specific seismic hazard evaluations performed for critical facilities such as nuclear and other types of power plants, nuclear waste repositories, and dams. However, due to the very nature of site-specific studies, the evaluation of seismic hazards in the western U.S. has been focused on a relatively few localized areas distributed throughout the western half of the country. Characterizing ground shaking hazards on a large areal basis has generally been either on a national scale such as the probabilistic National Hazard Maps produced by the U.S. Geological Survey (USGS) (Frankel *et al.*, 2002) or on a state-wide basis such as the maps produced for a few state departments of transportation (e.g., California, Arizona, and Oregon). Also, because of the large-scale nature of these maps, they are usually developed for a single geologic site condition, i.e., rock. Ground shaking hazard maps on a smaller scale such as might be developed for an urban metropolitan area or which incorporate the actual near-surface geology have with very few exceptions, not been developed for areas outside California. Urban ground shaking hazard maps are currently being developed for the Oakland, California; Seattle, Washington; and Memphis, Tennessee, urban areas by the USGS.

[1] Seismic Hazards Group, URS Corporation, 1333 Broadway, Suite 800, Oakland, CA 94612
[2] Pacific Engineering & Analysis, 311 Pomona Avenue, El Cerrito, CA 94530

Since 1997, we have developed deterministic earthquake scenario and probabilistic microzonation maps for strong ground shaking for areas throughout the U.S. including the Portland, Oregon, and the Salt Lake City, Utah, metropolitan areas and the Albuquerque-Belen-Santa Fe urban corridor in New Mexico, and the Salt Lake City-Ogden-Provo urban corridor in Utah. We also developed state maps for South Carolina and Montana. Our maps provide a quantitative measure of ground shaking and are of value to the engineering, urban planning, emergency preparedness and response communities, and the general public. A principal objective of these maps is to raise the public awareness of earthquake hazards in a given area. The maps can be used for loss estimation employing, for example, the HAZUS methodology or planning scenarios for emergency response. The intent of the maps is not to replace the USGS National Hazard Maps, which form the basis for U.S. building codes or site-specific studies particularly for important or critical facilities. Because the maps are for the ground surface, engineers relying solely on a building code-based approach will be able to evaluate the adequacy of their design levels (assuming inclusion of the site factors) by comparing them against the mapped values.

The ground motion parameters illustrated on the hazard maps are parameters of engineering and building code relevance: peak horizontal ground acceleration (PGA) and horizontal spectral accelerations (SA) at periods of 0.2 and 1.0 sec. The deterministic microzonation maps are for one to four earthquake scenarios. The probabilistic maps are generally for return periods of 500 and 2,500 years (10% and 2% exceedance in 50 years, respectively). The maps are for the ground surface and thus they incorporate the site response effects on ground shaking. The most up-to-date information on seismic sources, path effects, and near-surface geology are incorporated into the deterministic and probabilistic seismic hazard analyses. To address the wide range of interpretations and values as well as uncertainties of the input parameters, the latter are performed using a logic tree approach. The maps are produced using a raster-based GIS and are at scales of 1:24,000 to 1:1,000,000.

Methodology and Input to Hazard Calculations

There are generally six principal tasks that are required to produce hazard maps: (1) seismic source characterization; (2) definition and characterization of geologic site response categories; (3) site response analyses and calculation of amplification factors; (4) seismic attenuation characterization; (5) deterministic and/or probabilistic ground motion calculations; and (6) map development.

Seismic Source Characterization

The first step in any assessment of earthquake ground-shaking hazards is a characterization of the seismic sources that will produce ground motions of engineering significance at the site or area of interest. Seismic source characterization is concerned with three fundamental elements: (1) the identification, location, and geometry of significant source of earthquakes; (2) the maximum size distribution of earthquakes for each source; and (3) for probabilistic hazard, the rate at which different size earthquakes occur in each source. Parameters needed in a deterministic analysis include fault location, geometry, orientation, sense of slip, and maximum earthquake magnitude (M_{max}). In probabilistic hazard analyses, all these parameters are needed including recurrence model and rate. Uncertainties in the seismic source parameters are incorporated into probabilistic seismic hazard analysis using a logic tree approach. In this procedure, alternate models and/or the continuous distribution of source parameters are represented on multiple branches of logic trees with discrete characteristics and/or values and assigned weights.

In a probabilistic hazard assessment of earthquake ground motions, all seismic sources that can generate significant ground shaking at a site (generally those within a distance of 100 to 200 km in the western U.S.) are characterized. Two general types of seismic sources were considered in the probabilistic hazard analysis: active or seismogenic faults and background earthquakes.

Quaternary Faults

We generally include all known faults with evidence for repeated Quaternary movement as potential seismic sources. Where the data permit, we have attempted to consider and accommodate the structural variations that are potentially significant to hazard analysis by including a variety of rupture behavior models and fault geometries in our source characterization. Most faults are included as single independent (unsegmented) planar sources, unless the available data suggest otherwise. Zones of faults are modeled as multiple, distributed, parallel fault planes. Some faults show compelling evidence for being segmented, where relatively persistent segment boundaries have apparently confined prehistoric surface ruptures to particular sections of the faults. Finally, we note that the rupture behavior of many faults is poorly understood and is likely more complex than our simplifying assumptions. Faults are assumed to extend the full depth of the seismogenic crust, and so fault dips are averages estimated over the full depth of the seismogenic crust.

M_{max} values are estimated using the empirical relationships of Wells and Coppersmith (1994) for all fault types. Magnitudes were generally solely based on fault lengths, but we also considered displacements per event where data were available. In our analysis, we include distributions of $\pm$ 0.3 magnitude units around the preferred M_{max} to account for both aleatory and epistemic variabilities in determining M_{max} for faults, including uncertainties associated with the regression relations used and the input parameters to those relations, insofar as uncertainties in lengths and/or displacements were not explicitly included.

In assigning probabilities of activity for each fault source, we considered both the likelihood that it is structurally capable of independently generating earthquakes (seismogenic), and the likelihood that it is still active within the modern stress field. We incorporated many factors in assessing these likelihoods, such as: orientation in the modern stress field, fault geometry (length, continuity, depth extent, and dip), relation to other faults, age of youngest movement rates of activity, geomorphic expression, amount of cumulative offset, and any evidence for non-tectonic origin. The probability of activity for faults that do not show definitive evidence for repeated seismogenic Quaternary activity was individually judged based on available data and is discussed in more detail in our previous studies.

We considered truncated-exponential, characteristic, and maximum-magnitude recurrence models, with weights dependent on the fault length, type of data used to calculate activity rates, and type of rupture model. Observations of historical seismicity and paleoseismic investigations worldwide suggest that characteristic behavior is more likely for individual faults, whereas seismicity in zones best fits a truncated exponential model. Therefore, except for zones of faults, we generally favored the characteristic model of Youngs and Coppersmith (1985) for all fault sources.

We incorporate all available intermediate- (≤ 1.6 Ma) and short-term (≤ 130 ka) slip rate and/or recurrence interval data in characterizing rates of fault activity, but we generally prefer short-term recurrence interval data when available (Wong and Olig 1998). Rates are generally the most important fault parameters in hazard evaluation, but unfortunately most faults lack specific rate data. Compounding this difficulty is that many faults that have been studied show large variations in rates through time and in space. Depending on the available data, we have used a variety of approaches to characterize fault activity rates and their large uncertainties including: statistical analyses (e.g., McCalpin and Nishenko 1996 used in Wong *et al.* 2002), ergodic analyses that substitute space for time (e.g., McCalpin 1995 used in Wong *et al.* 2004), and geomorphic analyses and analogue comparisons (e.g., Ruleman 2002 and Anderson *et al.* 2005 used in Wong *et al.* 2005). Details of these approaches can be found in our previous studies. We have found no panacea for this problem and it will only be resolved by more study and better data on fault activity rates. Over the past 20 years we have also found that incorporating uncertainties significantly impacts the hazard and investigators typically underestimate both epistemic and aleatory uncertainties so we strive to avoid this pitfall.

Background Seismicity

The hazard from background (floating or random) earthquakes that are not associated with known or mapped faults needs to be incorporated into probabilistic hazard analysis. Earthquake recurrence estimates in the study region and M_{max} are required to assess the hazard from background earthquakes. In most of the western U.S., particularly the Basin and Range Province, the M_{max} for background earthquakes is about **M** 6½. Repeated events larger than these magnitudes probably produce recognizable fault-or fold-related features at the earth's surface (e.g., dePolo 1994). We usually adopt values of **M** 6¼ to 6¾ ± ¼ depending on the seismotectonic setting. The lower value is used in regions where the seismogenic crust tends to be thinner (< 15 km), i.e., regions characterized by higher than average heat flow. Conversely, higher M_{max} is used in regions with thicker seismogenic crusts such as the forearc of the Cascadia subduction zone (e.g., western Oregon).

In addition to the traditional approach of using areal source zones (assuming uniformly distributed seismicity), Gaussian smoothing (Frankel 1995) is used to address the hazard from background earthquakes in the probabilistic analysis. In this approach, we smooth the historical background seismicity to incorporate a degree of stationarity, using a spatial window of 15 km.

Geologic Site Response Units and Amplification Factors

In order to quantify the site response of soil and unconsolidated sediments, a shear-wave velocity profile, depth to a reference rock datum, and nonlinear dynamic material properties (both shear modulus reduction and damping curves as a function of shear strain) are required to define geologic site response categories. Based on these site response categories, frequency- and strain-dependent amplification factors can be computed. Site response categories are defined based on physical and dynamic properties of the materials. For example, the predominant units in Salt Lake Valley are lacustrine-alluvial silt and clay, lacustrine sand, and lacustrine gravel (Wong *et al.* 2002a).

We compute amplification factors as a function of site-response unit, ranges in thickness of the unconsolidated sediments, and input rock motion. Based on each average profile, 30 randomized profiles are computed to account for the horizontal and vertical variability in velocities and these were used in the simulations. The randomization is done using a correlation model for soil velocity profiles developed by Gabriel Toro (Risk Engineering Inc.). Shear modulus reduction and damping curves are assigned to the various site-response units to account for strain-dependent non-linear soil response.

We use the stochastic point-source numerical ground motion modeling approach coupled with an equivalent-linear methodology (Silva *et al.* 1997) to calculate amplification factors for 5%-damped response spectra for each site category. The point-source stochastic methodology is used to generate rock acceleration response spectra for a **M** 6.5 earthquake, which were then propagated up through the site-category profiles. The **M** 6.5 event is placed at several distances to produce input peak accelerations of 0.05, 0.10, 0.20, 0.40, 0.50, and 0.75 g. Thus the amplification factors (the ratios of the response spectra at the top of the profiles to the input spectra) are a function of the reference rock peak acceleration, spectral frequency, and non-linear soil response. Interpolation is used to obtain amplification factors at other reference rock peak accelerations.

Ground Motion Attenuation Characterization

To characterize the attenuation of ground motions, we use empirical attenuation relationships appropriate for soft rock sites in the western U.S. and the point-source stochastic numerical ground motion modeling technique to develop regions-specific relationships. We use empirical soft rock relationships such as: Abrahamson and Silva (1997), Spudich *et al.* (1999), Sadigh *et al.* (1997), and Campbell and Bozorgnia (2003). Relationships such as Youngs *et al.* (1997) were used in the Portland area for subduction zone earthquakes.

To compensate for the lack of region-specific attenuation relationships, stochastic modeling is used to model earthquakes of **M** 5.5, 6.5, and 7.5 in the distance range of 1 to 400 km. Uncertainties in stress drop, magnitude-dependent focal depths, the crustal attenuation parameters Q_o and η, the near-surface attenuation parameter (kappa), and the rock profile atop the crustal model are included in the computations of the attenuation relationships through parametric variations. Ranges of magnitude-dependent stress drops appropriate for extensional or compressional regimes are used. The aleatory variabilities in ground motion attenuation is included in the probabilistic analysis by using the log-normal distribution about the median values as defined by the standard error associated with each attenuation relationship. Three standard deviations about the median value are included in the analysis.

Scenario Ground Motions Calculations

The scenario ground motions are calculated using both empirical attenuation relationships and the stochastic finite-fault methodology (Silva *et al.* 1997). The latter explicitly incorporates the effects of the seismic source (fault geometry and dip, depth of rupture initiation, and sense of slip) and rupture propagation (e.g., directivity), which are particularly important at close distances to the fault. A total of 30 simulations are made where the slip models and rupture initiation are varied. We use the same values of Q_o and η in the scenario calculations as those assumed for the stochastic attenuation relationships. Scenario ground motion values are calculated by assigning a 0.40 weight to the values from the empirical attenuation relationships and 0.60 weight to the values from the stochastic finite-fault model. Total aleatory variability is estimated by combining the parametric and modeling variability (Silva *et al.* 1997) based on modeling recorded ground motions.

Probabilistic Seismic Hazard Analysis

To calculate the probabilistic ground motions, we perform comprehensive Cornell (1968) hazard analysis using logic trees. All known seismic sources that could generate strong ground shaking in the state, were incorporated into the probabilistic analysis. Both published empirical and stochastic attenuation relationships are used in the analyses to calculate the ground motion values. The mean probabilistic hazard is calculated at selected return periods.

Map Development

The ground shaking maps are produced using a vector- and raster-based GIS. Probabilistic ground motions on rock are calculated for the map areas using a grid of points at variable spacings of 5 to 20 km. Each grid point is assigned to a site response category. Surface ground motions are calculated by multiplying the rock ground motions by the appropriate amplification factors. The amplification factors for each grid point are selected based on the site response unit, depth to rock, and the input rock peak acceleration as described above. Based on grid of computed ground motions, values are interpreted at a spacing of 1 km. For each map, the peak or spectral acceleration values are then color contoured by interpolation in intervals of 0.10 g. The intent is to avoid implying a greater level of resolution and/or accuracy than was possible given the limitations of available geologic data.

Maps

Portland, Oregon Metropolitan Area

The Portland metropolitan area and surrounding vicinity have been the most seismically active region in Oregon in historical times. Based on the relatively brief 150-year historic record, six earthquakes of Richter magnitude (M_L) 5 or greater have occurred within the greater Portland area. In contrast, recent geophysical studies indicate the presence of at least three crustal faults beneath the Portland metropolitan area, which could generate much more damaging crustal earthquakes of M_L 6.5 or larger. Additionally, a convincing case has now been made to indicate that Cascadia subduction zone earthquakes up to **M** 9 in size have occurred in the prehistoric past, as recently as the year 1700, and will occur in the future. We have developed the first quantitative earthquake scenario and probabilistic microzonation maps for ground shaking for the Portland metropolitan area (Wong *et al.* 2000a, 2000b). These maps display color-contoured ground motion values in terms of PGA and horizontal SA at 0.2 and 1.0 sec periods. The maps depict ground shaking at the ground surface and thus incorporate the site-response effects of soils, unconsolidated sediments, and shallow rock. The scenario maps are for a **M** 9.0 earthquake along the megathrust of the Cascadia subduction zone and a hypothetical **M** 6.8 event on the Portland Hills fault. The probabilistic maps are for the two return periods of building code relevance, 500 and 2,500 years. The maps were funded by the USGS through the National Earthquake Hazard Reduction Program (NEHRP) External Grants Program.

Salt Lake City, Utah Metropolitan Area

The Salt Lake City metropolitan area is one of the most seismically hazardous urban areas in the interior of the western U.S. because of its location within the Intermountain Seismic Belt and its position adjacent to the active Wasatch fault. The elapsed time since the last large earthquake on the Salt Lake City segment of the Wasatch fault is approaching the mean recurrence interval based on the short-term paleoseismic record. We have developed nine microzonation maps showing surficial ground-shaking hazard (Wong *et al.* 2002a, 2002b). The maps incorporate the site response effects of the unconsolidated sediments that underlie most of the metropolitan are within Salt Lake Valley. These nine maps, at a scale of 1:75,000, make up three sets, each consisting of three maps that display color-contoured ground motion in terms of PGA and horizontal SA at periods 0.2 and 1.0 sec. One set of maps consists of "scenario" maps for a **M** 7.0 earthquake on the Salt Lake City segment of the Wasatch fault. The two other sets are probabilistic maps for the two return periods of 500 and 2,500 years. The maps were supported by the USGS NEHRP External Grants Program.

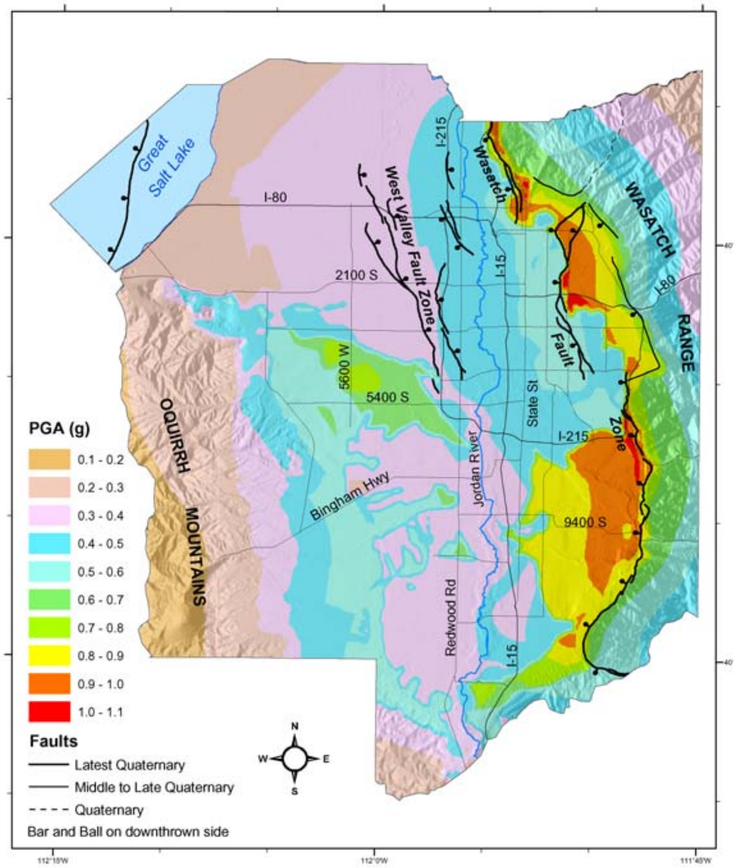

Figure 1. Salt Lake City segment, Wasatch fault **M** 7.0 earthquake scenario, peak horizontal acceleration (g) at the ground surface (Wong and others, 2002a).

Albuquerque-Santa Fe-Belen, New Mexico Urban Corridor

New Mexico's population is concentrated along the corridor that extends from Belen in the south to Española in the north and includes the cities of Albuquerque and Santa Fe. The Rio Grande rift, which encompasses the corridor, is a major tectonically, volcanically, and seismically active continental rift in the western U.S. Although only one large earthquake (**M** $\geq$ 6) has possibly occurred in the New Mexico portion of the rift since 1849, paleoseismic data indicate that prehistoric surface-faulting earthquakes of **M** 6.5 and greater have occurred on average every 400 years on many faults throughout the Rio Grande rift. Funded by the USGS NEHRP External Grants Program, we have developed a series of nine scenario and probabilistic hazard maps that portray the ground shaking that could occur in the Albuquerque-Belen-Santa Fe corridor from future earthquakes in New Mexico (Wong *et al.* 2004). These maps, at a scale of 1:500,000, display color-contoured ground-motion values in terms of the parameters of PGA and horizontal SA at 0.2 and 1.0 sec periods. The maps depict surficial ground shaking and incorporate the site-response effects at locations underlain by unconsolidated sediments. The scenario maps are for a **M** 7.0 earthquake rupturing the Sandia-Rincon faults, which are adjacent to and dip west beneath Albuquerque. The probabilistic maps are for return periods of 500 and 2,500 years.

Salt Lake City-Ogden-Provo, Utah Urban Corridor

As part of a study to characterize the seismic hazards along the populated Wasatch Front extending from Ogden south to Provo, including the Salt Lake City metropolitan area, we have developed three scenario ground shaking hazard microzonation maps (Solomon *et al.* 2004). The scenario maps display the ground motions that would result from a **M** 7.0 earthquake occurring on the Salt Lake City segment of the Wasatch fault. The scenario ground motions were then used in assessments of liquefaction potential and earthquake-induced landsliding for the mapped area (Solomon *et al.* 2004). The maps incorporate the site response effects of the soils and unconsolidated sediments that exist in the valleys adjacent to the Wasatch fault and in the back valleys in the Wasatch Range. The maps are expressed in terms of PGA and horizontal SA at periods of 0.2 and 1.0 sec. The frequency-dependent pattern of both amplification and deamplification in the map area is clearly a function of the distribution and thickness of the surficial geologic units. Hanging wall effects are also evident on the hazard maps but are masked to a large extent by the site effects. The maps were funded by the USGS NEHRP External Grants Program.

South Carolina

On 31 August 1886, an earthquake of approximate **M** 7 struck Charleston, South Carolina. The event not only damaged or destroyed the large majority of buildings in the City of Charleston but caused widespread damage throughout much of the southeastern U.S. A future repeat of this earthquake would be a national catastrophe (Wong *et al.* 2005a). As part of a comprehensive earthquake loss and vulnerability evaluation of the state of South Carolina funded by the South Carolina Emergency Preparedness Division and FEMA, scenario ground motion maps were developed for a **M** 7.3 “1886 Charleston-like” earthquake using finite-fault and point-source stochastic numerical modeling (Silva *et al.* 2003). Because there is considerable uncertainty regarding the 1886 source, the rupture plane of the 1886 event was modeled as both a 100-km-long, 20-km-wide fault (static stress drop of 27 bars) and a 50-km-long, 16-km-wide fault (107-bar stress drop). The source was assumed to be a north-northeast-striking, strike-slip fault coincident with the Woodstock fault. Statewide maps were developed for the ground surface and PGA, 0.3 sec and 1.0 sec SA, and peak ground velocity so they could be input into the loss estimation program HAZUS (Wong *et al.* 2005a). Scenario maps for **M** 6.3 and **M** 5.3 earthquakes along the 1886 source and a **M** 5.3 in Columbia were also developed.

Montana

Hazard maps are a useful tool for regulatory agencies responsible for the seismic safety of important and critical facilities, particularly if their inventory is large and their area large and geologically and seismically diverse. Western Montana, located in the northern Intermountain region of the U.S., is characterized by abundant late-Quaternary Basin and Range normal faulting and historical seismicity. The largest historical event was the 1959 **M** 7.3 Hebgen Lake earthquake, located west of Yellowstone National Park. In contrast to western Montana, eastern Montana has only two known faults of possible late-Quaternary age. Seismicity is at a relatively low level, although the largest event may have been about **M** 5.5. Because of the potential earthquake threat to dams in the State, probabilistic earthquake ground motion maps have been developed for the Montana Department of Natural Resources and Conservation (DNRC) Dam Safety Program (Wong *et al.* 2005b). The 18 statewide maps display PGA and 0.2 and 1.0 sec horizontal SA for return periods of 500, 2,500, and 5,000 years. The maps display ground motions for two site conditions: soft rock and the ground surface. In addition to the ground shaking maps, a set of 6 maps have been developed to aid DNRC and practicing engineers in the analysis of site response and liquefaction potential. These maps display the modal earthquake magnitude and modal distance of the magnitude–distance distribution that contributes to the hazard at a specified location for the three return periods. The maps were funded by DNRC and FEMA.

Acknowledgments

We would like to acknowledge the contributions of many individuals who assisted in the preparation of these maps but in particular Melinda Lee, Robyn Schapiro, Jacqueline Bott, Anna Sojourner, and Eliza Nemser. Our gratitude to the USGS NEHRP External Grants Program, FEMA, and the state geological surveys of Oregon, Utah, New Mexico, and Montana for their support of our mapping efforts.

References

Abrahamson, N.A., and W.J. Silva, 1997. Empirical Response Spectral Attenuation Relations for Shallow Crustal Earthquakes. *Seismological Research Letters*, 68, 94-127.

Anderson, L.W., L.A. Piety, S.S. Olig, and S.L. Forman, 2005. Paleoseismic Investigation of the Canyon Ferry Fault, West Central Montana. In *Proceedings of Basin and Range Province Seismic Hazards Summit II*, edited by W.R. Lund. Utah Geological Survey Miscellaneous Publication 05-2 (CD-ROM).

Campbell, K.W., and Y. Bozorgnia, 2003. Updated Near-Source Ground Motion (Attenuation) Relations for the Horizontal and Vertical Components of Peak Ground Acceleration and Acceleration Response Spectra. *Bulletin of Seismological Society of America* 93, 314-331.

Cornell, C.A., 1968. Engineering Seismic Risk Analysis. *Bulletin of the Seismological Society of America* 58, 1583-1606.

dePolo, C.M., 1994. The Maximum Background Earthquake for the Basin and Range Province, Western North America. *Bulletin of the Seismological Society of America* 84, 466-472.

Doser, D.I., 1985. Source Parameters and Faulting Processes of the 1959 Hebgen Lake, Montana, Earthquake Sequence. *Journal of Geophysical Research* 90, 4537-4555.

Frankel, A., 1995. Mapping Seismic Hazard in the Central and Eastern United States. *Seismological Research Letters*, 66, 8-21.

Frankel, A., M. Peterson, C. Mueller, K. Haller, R. Wheeler, E. Leyendecker, R. Wesson, S. Harmsen, C. Cramer, D. Perkins, and K. Rukstales, 2002. “Documentation for the 2002 Update of the National Seismic Hazard Maps.” U.S. Geological Survey Open-File Report 02-420, 33 p.

McCalpin, J.P., 1995. Frequency Distribution of Geologically Determined Slip Rates for Normal Faults in the Western U.S. *Bulletin of the Seismological Society of America* 85, 1867-1872.

McCalpin, J.P., and S.P., Nishenko, 1996. Holocene Paleoseismicity, Temporal Clustering, and Probabilities of Future Large (M>7) Earthquakes on the Wasatch Fault Zone, Utah. *Journal of Geophysical Research* 101, 6,233-6,253.

Ruleman, Chester A., III, 2002. *Quaternary Tectonic Activity Within the Yellowstone Tectonic Parabola and Associated Seismic Hazards, Southwest Montana, Montana State University*. M.S. Thesis, 158 p., 3 plates.

Sadigh, K., C.-Y. Chang, J.A. Egan, F. Makdisi, and R.R. Youngs, 1997. Attenuation Relationships for Shallow Crustal Earthquakes Based on California Strong Motion Data. *Seismological Research Letters* 68, 180-189.

Silva, W.J., N.A. Abrahamson, G. Toro, and C. Constantino, 1997. *Description and Validation of the Stochastic Ground Motion Model*. Unpublished report prepared for the Brookhaven National Laboratory.

Silva, W., I. Wong, T. Siegel, N. Gregor, R. Darragh, and R. Lee, 2003. Ground Motion and Liquefaction Simulation of the 1886 Charleston, South Carolina, Earthquake. *Bulletin of the Seismological Society of America*, 93, 2717-2736.

Solomon, B.J., N. Storey, I. Wong, W. Silva, N. Gregor, D. Wright, and G. McDonald, 2004. Earthquake-"Hazards Scenario for a **M** 7 Earthquake Along the Salt Lake City Segment of the Wasatch Fault Zone, Utah." Utah Geological Survey Special Study SS-111 DM (CD-ROM).

Spudich, P., W.B. Joyner, A.G. Lindh, D.M. Boore, B.M. Margaris, and J.B. Fletcher, 1999. SEA99 - A Revised Ground Motion Prediction Relation for use in Extensional Tectonic Regimes. *Bulletin of the Seismological Society of America* 89, 1156-1170.

Wells, D.L., and K.J. Coppersmith, 1994. New Empirical Relationships Among Magnitude, Rupture Length, Rupture Width, Rupture Area, and Surface Displacement. *Bulletin of the Seismological Society of America* 84, 974-1002.

Wong, I., J. Bouabid, W. Graf, C. Huyck, A. Porush, W. Silva, T. Siegel, G. Bureau, R. Eguchi, and J. Knight, 2005a. Potential Losses in a Repeat of the 1886 Charleston, South Carolina, Earthquake. *Earthquake Spectra* (in press).

Wong, I.G., and Olig, S.S., 1998. Seismic Hazards in the Basin and Range Province: Perspectives from Probabilistic Analyses. In *Proceedings Volume, Basin and Range Province Seismic-Hazards Summit*, edited by W.R. Lund. Utah Geological Survey Miscellaneous Publication 98-2, 110–127.

Wong, I., S. Olig, M. Dober, W. Silva, D. Wright, P. Thomas, N. Gregor, A. Sanford, K-W. Lin, and D. Love, 2004. Earthquake Scenario and Probabilistic Ground Shaking Hazard Maps for the Albuquerque-Belen-Santa Fe, New Mexico Corridor. *New Mexico Geology*, 26, 3-35.

Wong, I., S. Olig, M. Dober, D. Wright, E. Nemser, D. Lageson, W. Silva, M. Stickney, M. Lemieux, and L. Anderson, 2005b. "Probabilistic Earthquake Hazard Maps for the State of Montana." Montana Bureau of Mines and Geology, Special Publication 117, 72 p.

Wong, I., W. Silva, J. Bott, D. Wright, P. Thomas, N. Gregor, S. Li, M. Mabey, A. Sojourner, and Y. Wang, 2000a. "Earthquake Scenario Ground Shaking Map for the Portland, Oregon, Metropolitan Area, Portland Hills Fault **M** 6.8 Earthquake, Peak Horizontal Acceleration (g) at the Ground Surface." Oregon Department of Geology and Mineral Industries Interpretative Map Series IMS-15, scale 1:62,500.

Wong, I., W. Silva, J. Bott, D. Wright, P. Thomas, N. Gregor, S. Li, M. Mabey, A. Sojourner, and Y. Wang, 2000b. "Earthquake Scenario and Probabilistic Ground Shaking Maps for the Portland, Oregon, Metropolitan Area." Oregon Department of Geology and Mineral Industries Interpretive Map Series IMS-16, scale 1:62,500, 11 sheets with 16 p. text.

Wong I., W. Silva, S. Olig, P. Thomas, D. Wright, F. Ashland, N. Gregor, J. Pechmann, M. Dober, G. Christenson, R. Gerth, 2002a. "Earthquake Scenario and Probabilistic Ground Shaking Maps for the Salt Lake City, Utah, Metropolitan Area." Utah Geological Survey Miscellaneous Publication MP-02-05, 50 p.

Wong, I., W. Silva, D. Wright, S. Olig, F. Ashland, N. Gregor, G. Christenson, J. Pechmann, P. Thomas, M. Dober, and R. Gerth, 2002b. "Ground Shaking Map for a Magnitude 7.0 Earthquake on the Wasatch Fault, Salt Lake City, Utah, Metropolitan Area, Utah Geological Survey Public Information Series 76.

Youngs, R.R., S.-J. Chiou, W.J. Silva, and J.R. Humphrey, 1997. Strong Ground Motion Attenuation Relationships for Subduction Zone Earthquakes. *Seismological Research Letters*, 68, 58-73.

Youngs, R.R. and K.J. Coppersmith, 1985. Implications of Fault Slip Rates and Earthquake Recurrence Models to Probabilistic Seismic Hazard Estimates. *Bulletin of the Seismological Society of America* 75, 939-964.